Novel Ultra Thin Gate Oxide Growth Technique by Alternating Current Anodization

Jenn-Gwo Hwu*, Chuang-Yuan Lee, Chieh-Chih Ting, and Wei-Len Chen
Room 446, Department of Electrical Engineering/
Graduate Institute of Electronics Engineering,
National Taiwan University, Taipei, Taiwan, Chinese Taipei
*E-mail: hwu@cc.ee.ntu.edu.tw, Fax: 886-2-23671909, Tel: 886-2-23635251 ext. 446

Abstract

Ultra-thin gate oxides prepared by the novel anodic oxidation technique of using direct-current (DC), alternating-current (AC), and direct-current with ac oscillation (DAC) as anodization voltages are studied. After suitable high temperature anneal in N_2, these anodic oxides (ANO) show improved uniformity in electrical characteristics with respect to conventional rapid thermal oxides. Smaller leakage current and higher breakdown endurance are observed for these ANO oxides. Specially, DAC-ANO oxides present a further improved breakdown performance than the other oxides. Further, anodization is carried out with N-type Si (ANO-Si) replacing Pt as the cathode. ANO-Si oxides demonstrate even preferable reliability and superior electrical uniformity.

Introduction

Thin gate oxides with thickness smaller than 30 Å are needed in the future technology. The large direct tunneling current in such thin oxides is a key issue in the consideration of device scaling. Because of the disadvantages of non-uniform temperature distribution, thermal stress and dopant diffusion in high temperature processing, the growing need for alternatives to high-temperature thermal gate oxide is enhanced [1]. It was also noted that better thickness uniformity leads to more optimistic projection of oxide reliability [2]. It had been demonstrated of the manufacturing feasibility of uniform 1.5 nm gate oxides with a standard deviation of around 0.13 nm [3]. Anodization, featured as low-temperature processing, had been studied earlier [4-6]. Owing to the self-readjustment nature of current conduction through the weak path in the oxide during anodization [7], anodic oxides inherit the merits of less pinholes and better thickness uniformity. In addition, the anodic oxide followed by rapid thermal nitridation are of better quality than the rapid thermal oxide (RTO) due to nitrogen incorporation relieving interfacial strain and suppressing the interface-trap generation [8]. In this work, we use it as an alternative method to prepare ultra thin gate oxides.

Conventionally, anodization was carried out by applying a constant voltage or a constant current between the silicon wafer and the platinum cathode. Innovations of our work can be categorized into two respects. First, rather than direct-current anodization (DC-ANO) and alternating-current anodization (AC-ANO), direct-current with AC oscillation anodization (DAC-ANO) is proposed. Second, the N-type silicon cathode instead of the traditional platinum cathode is adopted for anodization to prepare high-quality ultra-thin gate oxides. Surprisingly, we found that the DAC-ANO oxides obtained using N-type Si wafer as cathode electrode exhibit a further improved uniformity in current density distribution.

Experiment

3-inch boron-doped P-type (100) silicon wafers are used as the substrates to fabricate metal-oxide-semiconductor (MOS) capacitors. After the standard RCA clean, the native oxide on the wafer is removed. Oxidation is then carried out by distinct anodization techniques in D.I. water and by rapid thermal oxidation (RTO) in O_2 ambient of 200 torrs at 850°C for 5 seconds. The designed voltage profiles applied to the anode silicon wafers and the experimental setups for DC-ANO, AC-ANO and DAC-ANO are illustrated in Fig.1. It is noted that in addition to the Pt cathode, the phosphorus-doped N-type (100) silicon wafer is also used as the cathode for anodization; they are denoted as ANO-Pt and ANO-Si, respectively. All anodic oxides are treated with post oxidation annealing (POA) in N_2 ambient of 200 torrs at 850°C for 20 seconds. Following this, aluminum films are evaporated on the oxides and the photolithography is performed to pattern 150 μm × 150 μm metal gates. Last, aluminum films are evaporated again as the back contacts of the MOS capacitors.

Results and discussions

It is known that in D.I. water, H^+ cations and OH^-

0-7803-6520-8/01/$10.00 © 2001 IEEE.

anions are existed in the electrolyte as shown in Fig.2. During anodization, OH^- anions were drifted toward the anode electrode to react with Si substrate to become SiO_2. A leaky path will suffer a higher electric field and therefore a higher oxidation rate. So, it is believed that self-readjustment nature is existed in the ANO oxides.

A. DC-ANO (ANO-Pt)

Figure 3 shows the J-V curves of DC-ANO and RTO oxides. Clearly, ANO oxides have smaller leakage currents than RTO ones. Figure 4(a) and (b) show the FTIR spectrum of an ANO oxide before and after 900°C annealing, respectively. It demonstrates that a suitable high temperature anneal is necessary to remove most of the hydrogen related to defects in ANO oxides. Figure 5 shows the FN plots of DC-ANO and RTO oxides. A barrier height of 3.34eV at metal/SiO_2 interface was found for ANO oxide. This higher barrier height is related to the negative charges from anions. This is one possible reason for the smaller gate injection current observed in ANO oxides. Another reason for the above observation is that the ANO oxides have a more uniform thickness distribution than RTO ones. Figure 6 shows the theoretical simulation of a capacitor with composite oxides. With a simplified assumption of two areas in parallel, one can see that a small portion of local thin region will make the total device current level high and close to the thin oxide behavior. So, a more uniform oxide thickness distribution such as ANO oxides should have a smaller leakage current in comparison with the RTO oxides with the same thickness as measured by ellipsometer.

B. AC-ANO (ANO-Pt)

It is observed in Fig.7 that oxides prepared at 200Hz are more uniform than those at 0.2Hz. The Weibull plots of TZDB are exhibited in Fig.8. Obviously, all ANO oxides, especially the AC-ANO ones, demonstrate better breakdown performance than the RTO oxide. Moreover, AC20Hz, AC200Hz, and AC2KHz present even higher breakdown fields than AC0.2Hz. The TDDB performance is also improved by high-frequency AC-ANO as shown in Fig.9. However, the J-V curves in Fig.10 reveal that as the gate voltage under substrate injection increases, the currents of the AC200Hz devices slowly increase toward saturation, while most of the AC2KHz devices break down. The inset of Fig.10 summarizes the saturation and breakdown percentage at 6V bias. Consequently, AC200Hz oxide exhibits lower D_{it} than AC2KHz one.

It is believed that the compensation effect by ion redistribution contributes to improved thickness uniformity and preferable breakdown endurance of AC-ANO oxides. During AC-ANO, the voltage polarity connected to the silicon wafer is periodically changed. When the voltage is switched from positive to negative, $(OH)^-$ ions reverse to the Pt plate; when it comes to positive polarity again, $(OH)^-$ ions are redistributed and adjust their moving directions to those leakier paths. Reiteration of reversing the voltage polarity increases the probability of reducing leaky paths in the oxide and this remedy dominates at a higher switching frequency.

C. DAC-ANO (ANO-Pt)

Figure 11 shows the C-V curves of DAC-ANO oxides. The accumulation and inversion behavior for DAC-ANO oxides are quite good for an insulator in 20 Å thickness. The Weibull plots of TZDB in Fig.12 show that all DAC-ANO oxides are of larger breakdown fields than the DC-ANO oxide and 5V is found to be the optimal AC oscillation amplitude. Fig.13 further displays that DAC-ANO oxide is much more endurable to the electrical stress than DC-ANO oxide. This improved breakdown performance suggests that the AC oscillation superposed on the DC anodization voltage can assist in repairing oxide leakage paths through voltage switching.

For DAC-ANO, the voltage applied to the wafer is composed of two components, a DC bias and an AC signal. The DC bias serves as the anodization voltage and the superposed AC oscillation is endowed with the compensation effect by anion redistribution. Therefore, DAC-ANO prepares equally high-quality oxide due to the AC oscillation, and is more time-efficient than the AC-ANO technique due to the positive DC bias.

D. ANO-Si

To avoid metal contamination, anodization is carried out for the first time with the N-type Si wafer as the cathode. Oxides of varied thicknesses are systematically grown by the DAC-Si technique and their J-V and C-V characteristics are investigated in Figs.14 and 15, respectively. It is noted that the leakage current density of 3.66×10^{-3} A/cm^2 at –3V bias for 18Å DAC-Si oxide is even less than that of 8.58×10^{-3} A/cm^2 for 20Å RTO oxide. The flat-band voltages (V_{FB}) of DAC-Si oxides range from –0.83 to –0.86 volt, and the V_{FB} of RTO oxide is –1.23 volt. This difference is attributed to some pre-trapped negative oxide charges in the anodic oxides as described in the previous section.

E. Comparison between ANO-Pt and ANO-Si

The comparison between DC-Pt, DC-Si, DAC-Pt, and DAC-Si are examined. Figure 16 shows the J-V curves of these samples with a thickness of about 20 Å. It was found the ANO-Si oxides have a little larger

current level than the ANO-Pt ones. The actual reason is unknown. However, the breakdown endurance of ANO-Si oxides is superior to that of ANO-Pt ones. Figure 17 (a) and (b) show the TZDB and TDDB data between them. By examining the positive bias J-V cures of these samples as shown in Fig.18, one can find that ANO-Si samples preserve less damage in Si surface than ANO-Pt ones since the former oxides have smaller saturation currents than the others.

The variations of the gate leakage current densities under the oxide voltage of –2V for 20Å oxides are displayed in Fig.19. ANO-Si oxides are of less current variations than ANO-Pt and RTO ones. It is suggested that the N-type Si wafer is less easily bent and deformed than the malleable Pt; therefore, the inherent non-uniformity of the field, between the anode and the cathode, is much reduced.

Finally, various ANO-Si oxides of 11 to 32Å are compared with ANO-Pt and RTO oxides in current density variation as shown in Fig.20. It was observed that ANO-Si oxides are of prime electrical uniformity. Figure 21 shows the FTIR spectrum for various ANO oxides. The peak signals for Si-O-Si stretching mode are almost the same for all the ANO oxides.

Conclusion

Several novel anodization techniques for thin gate oxide growth are proposed in this work. It is exhibited that AC-ANO and DAC-ANO oxides both present better breakdown endurance than DC-ANO and RTO oxides. Concerning AC-ANO methods, high-frequency AC-ANO oxide is more resistant to the electrical stress than low-frequency AC-ANO oxide. However, it is inspected that a high-frequency process may damage the bonding structure at the Si/SiO_2 interface, increasing the interface-trap density. 200Hz is found to be the optimal frequency. For DAC-ANO methods, it is observed that a small AC signal upon the DC bias voltage can greatly improve the oxide quality. It is believed that the compensation effect by anion redistribution in water during voltage switching is responsible for the superior characteristics of AC-ANO and DAC-ANO oxides. N-type Si is used as the cathode for anodization for the first time. It is perceived that ANO-Si oxides excel ANO-Pt ones in better reliability and greater electrical uniformity. It is therefore believed that ANO-Si is potential to be useful in the preparation of high-quality ultra-thin gate oxides.

Acknowledgments

The authors want to thank the National Science Council of ROC for supporting this work under contract No. NSC-89-2215-E002-042.

References

[1] K.B.Clark, J.A.Bardwell, and J.-M.Baribeau, *J. Appl. Phys.*, vol. 76, 3114 (1994).

[2] B. E. Weir, P. J. Silverman, M. A. Alam, F. Baumann, D. Monroe, A. Ghetti, J. D. Bude, G.L. Timp, A. Hamad, T.M. Oberdick, N.X. Zhao, Y. Ma, M.M. Brown, D. Hwang, T.W. Sorsch, and J. Madic, *IEDM Technical Digest*, (Washington, DC, USA, 1999) p.437.

[3] H.S. Momose, S. Nakamura, T. Ohguro, T. Yoshitomi, E. Morifuji, T. Morimoto, Y. Katsumata, and H. Iwai, *IEEE Trans. Electron Devices*, ED-45, 691(1998).

[4] G.C. Jain, A. Prasad, and B.C. Chakravarty, *J. Electrochem Soc.*, vol.126, 89 (1979)

[5] K. Ghowsi, and R.J. Gale, *J. Electrochem. Soc.*, vol.136, 867 (1989).

[6] S.K. Sharma, B.C. Chakravarty, S.N. Singh, B.K. Das, D.C. Parashar, J. Rai, and P.K. Gupta, *J. Phys. Chem. Solids*, vol.50, 679 (1989).

[7] M. J. Jeng and J. G. Hwu, *Appl. Phys. Lett.*, vol. 69, 3875 (1996).

[9] M. J. Jeng and J. G. Hwu, *IEEE Electron Device Lett.*, vol. 17, 575 (1996).

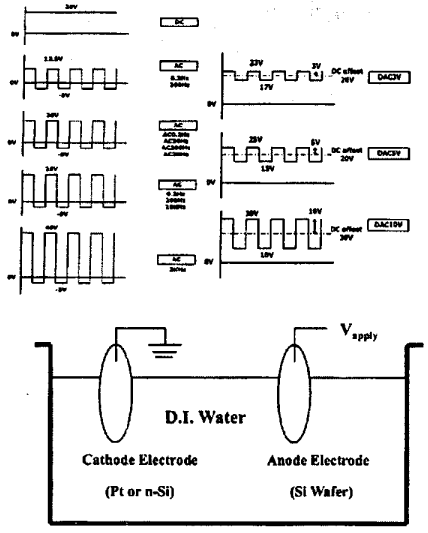

Fig.1: Experimental setup for anodic oxidation.

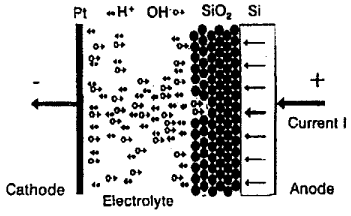

Fig.2: Self-readjustment nature of anodic oxide.

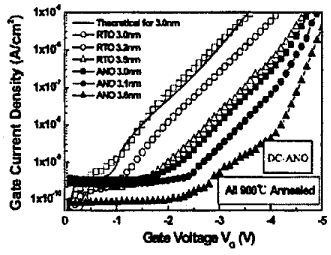

Fig.3: J-V curves of DC-ANO and RTO oxides.

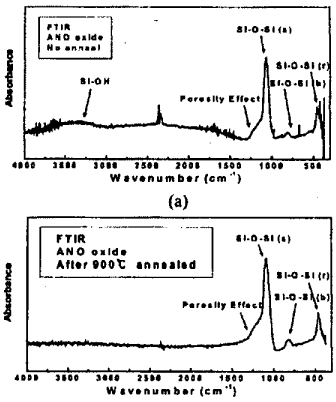

Fig.4: FTIR spectrum of an anodic oxide (a) before and (b) after 900°C anneal.

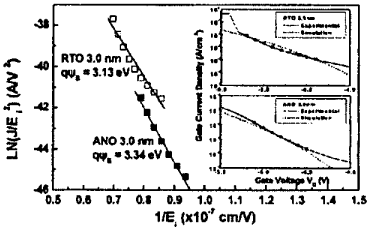

Fig.5: FN plots of DC-ANO and RTO oxides.

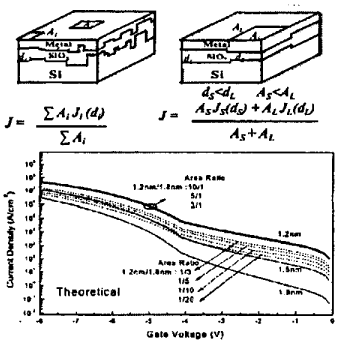

Fig.6:Theoretical J-V curves of composite oxides.

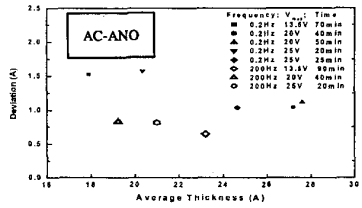

Fig.7: Effect of switching frequency on AC-ANO oxide thickness uniformity.

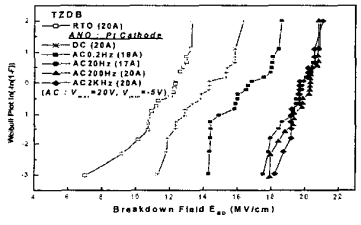

Fig.8: The Weibull plots of TZDB for AC-ANO, DC-ANO and RTO oxides.

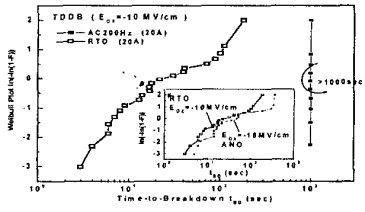

Fig.9: The Weibull plots of TDDB for AC-ANO and RTO oxides

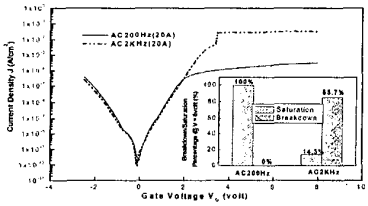

Fig.10: J-V curves and saturation/breakdown percentage at 6V for AC200Hz and AC2KHz-ANO oxides.

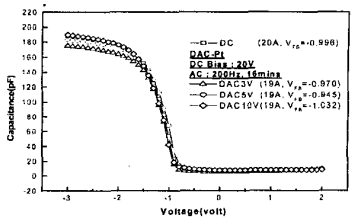

Fig.11: The C-V curves of DAC-ANO oxides.

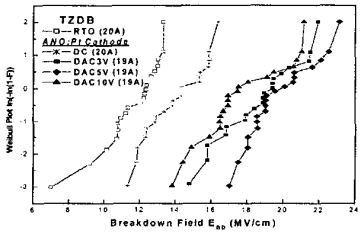

Fig.12: The Weibull plots of TZDB for DAC-ANO, DC-ANO, and RTO oxides.

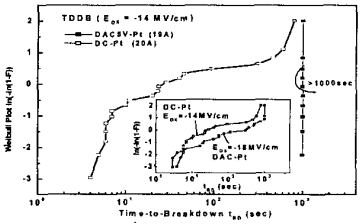

Fig.13: The Weibull plots of TDDB for DAC5V-ANO and DC-ANO oxides.

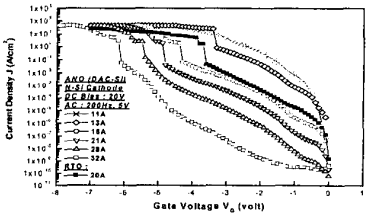

Fig.14: The J-V curves of DAC-Si and RTO oxides.

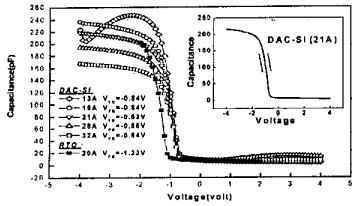

Fig.15: The C-V curves of DAC-Si and RTO oxides.

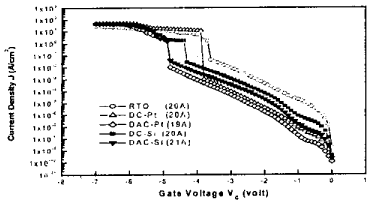

Fig.16: The J-V curves of DC-Pt, DAC-Pt, DC-Si, DAC-Si, and RTO oxides.

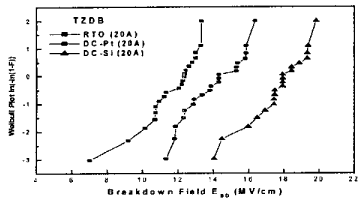

(a)

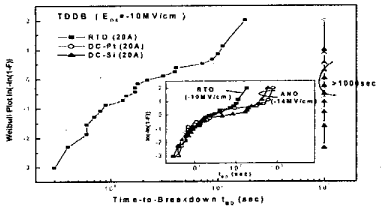

(b)

Fig.17: The Weibull plots of (a)TZDB and (b)TDDB for DC-Pt, DC-Si, and RTO oxides.

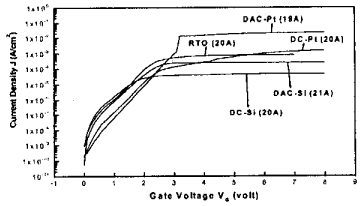

Fig.18: The positive bias J-V curves of DC-Pt, DAC-Pt, DC-Si, DAC-Si and RTO oxides.

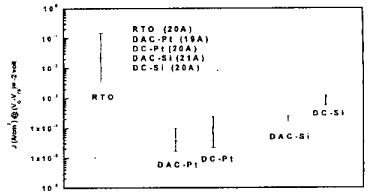

Fig.19: Variation of the leakage current for DC-Pt, DAC-Pt, DC-Si, DAC-Si and RTO oxides

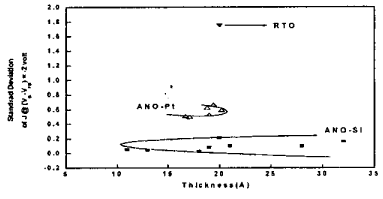

Fig.20: Current variation versus thickness for various ANO-Pt, ANO-Si, and RTO oxides.

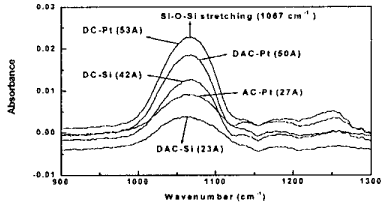

Fig.21. FTIR spectrum of various ANO oxides.